3-1-2015

Geometry Optimization of Uncoated Silicon Microcantilever-based Gas Density Sensors

M. T. Boudjiet
University of Bordeaux

J. Bertrand
Agence Nationale pour la Gestion des Déchets Radioactifs

F. Mathieur
Centre National de la Recherche Scientifique

L. Nicu
Centre National de la Recherche Scientifique

L. Mazenq
Centre National de la Recherche Scientifique

See next page for additional authors

Geometry optimization of uncoated silicon microcantilever-based gas density sensors

M.T. Boudjiet
Univ. Bordeaux, IMS
UMR 5218, F-33400 Talence, France

J. Bertrand
Andra
F-92298 Châtenay-Malabry, France

F. Mathieu
CNRS, LAAS
F-31077 Toulouse, France

L. Nicu
CNRS, LAAS
F-31077 Toulouse, France

L. Mazenq
CNRS, LAAS
F-31077 Toulouse, France

T. Leïchlé
CNRS, LAAS
F-31077 Toulouse, France

Sensors and Actuators B: Chemical, Vol. 208 (March 2015): pg. 600-607. DOI.

S.M. Heinrich
Department of Civil, Construction and Environmental Engineering, Marquette University
Milwaukee, WI

C. Pellet
Univ. Bordeaux, IMS
UMR 5218, F-33400 Talence, France

I. Dufour
Univ. Bordeaux, IMS
UMR 5218, F-33400 Talence, France

Abstract:

In the absence of coating, the only way to improve the sensitivity of silicon microcantilever-based density sensors is to optimize the device geometry. Based on this idea, several microcantilevers with different shapes (rectangular-, U- and T-shaped microstructures) and dimensions have been fabricated and tested in the presence of hydrogen/ nitrogen mixtures (H2/N2) of various concentrations ranging from 0.2% to 2%. In fact, it is demonstrated that wide and short rectangular cantilevers are more sensitive to gas density changes than U- and T-shaped devices of the same overall dimensions, and that the thickness doesn't affect the sensitivity despite the fact that it affects the resonant frequency. Moreover, because of the phase linearization method used for the natural frequency estimation, detection of a gas mass density change of 2 mg/l has been achieved with all three microstructures. In addition, noise measurements have been used to estimate a limit of detection of 0.11 mg/l for the gas mass density variation (corresponding to a concentration of 100 ppm of H2 in N2), which is much smaller than the current state of the art for uncoated mechanical resonators.

Keywords: Density sensor, hydrogen sensor, microcantilever, geometry optimization, sensitivity optimization, Euler-Bernoulli beam theory, hydrodynamic function.

Sensors and Actuators B: Chemical, Vol. 208 (March 2015): pg. 600-607. DOI.

1. Introduction

In recent years microcantilever-based chemical, biological and physical sensors have attracted the interest of numerous researchers due to their high surface-to-volume ratio and their high performance in both gas and liquid phases [1-6]. For chemical and biochemical sensing applications, the microcantilevers are usually coated with a sensitive layer whose purpose is to selectively sorb the analyte of interest, resulting in either a static deflection (bilayer effect) in the static mode or a shift in the resonant frequency (mass effect) in the dynamic flexural mode. Furthermore, it has been demonstrated that uncoated micro- or millimeter size cantilevers operated in the dynamic flexural mode exhibit good sensitivities to gas mass density [7,8], liquid mass density [9] and/or viscosity [10,11].

With a view towards chemical detection in gas media, the variation of the gas density can reflect the variation of a chemical species concentration in a gas mixture [8, 12-14]. The operating principle of an uncoated silicon microcantilever (USMC) used as a density or chemical sensor is based on the influence of the mass of the fluid moved by the vibrating cantilever on the resonant frequency. In fact, when the surrounding fluid mass density increases (decreases), the equivalent effective mass of the cantilever increases (decreases), thereby causing the resonant frequency to decrease (increase) [12].

The absence of a coating eliminates or significantly reduces several problems associated with microcantileverbased sensors such as long-time response, drift and aging effects. However, uncoated microcantilevers are nonselective and offer very low sensitivities, making it quite challenging to detect small concentration changes (small density changes). This last point serves as the motivation to increase the sensor sensitivity through geometry optimization.

In the literature geometry optimization has already been reported for other particular cases of chemical detectors. For example, in the static bending mode, A. Loui *et al.* [15] have studied the influence of the length-to-width aspect ratio on the sensitivity of rectangular cantilevers due to both surface stress and an end-force loading. They have found that structures with a low aspect ratio are better for surface-stress applications and structures with high aspect

Sensors and Actuators B: Chemical, Vol. 208 (March 2015): pg. 600-607. DOI.

ratio are optimal for point-loading scenarios. In the case of dynamic mode operation, the cantilever mass sensitivity is proportional to its resonant frequency. The resonant frequency is proportional to the square root of the stiffness and inversely proportional to the square root of the effective mass. Therefore, the majority of the studies conducted in order to improve the mass sensitivity of cantilevers are focusing on increasing the stiffness (*k*) and/or decreasing the effective mass (*meff*) using different methods. H. Hocheng *et al.* [16] have demonstrated using different microcantilever shapes that the higher the structural stiffness is, the better the sensitivity is. Similarly, S. Subramanian *et al.* [17] suggested the use of a nonlinear width profile for V-shaped microcantilevers in order to increase the structural stiffness and subsequently the mass sensitivity. For bio-sensing applications and in order to improve the overall (static-mode and dynamic-mode) sensitivity of a microcantilever, as measured by the product of static deflection and resonant frequency, M.Z. Ansari *et al.* [18] proposed using a non-uniform cantilever cross-section (giving increased *k* and decreased *meff*) and reducing the fixed-end area (increasing the static deflection). The authors suggested triangular or step cross-section profiles instead the conventional rectangular one. Another solution, proposed by M. Narducci *et al.* [19], consisted of reducing the microcantilever size (increasing *k* and reducing *meff*) and/or using higher-order modes. In the case of end-mass loading, S. Morshed *et al.* [20] have demonstrated via simulation studies that structures with high aspect ratio (length-to-width) are more sensitive to local end-mass variation; furthermore, they have suggested the use of a triangular microcantilever shape to enhance the stiffness and minimize the effective mass at the free-end of the structure. Furthermore, to enhance the capabilities of microcantilevers in liquid media, L.A. Beardslee *et al.* [21] have studied the influence of the beam geometry on both the quality factor and the resonant frequency in a liquid medium (water) in order to limit the viscous damping effect, thus improving the detection limit of chemical sensing. The authors reported that the use of the in-plane bending mode reduces the damping and the mass loading due to the surrounding fluid, and that beams that are wide, thin and short and operated in the in-plane mode are more suitable for liquid-phase chemical detection.

As reported above, the resonant frequency is a key parameter in determining the cantilever mass sensitivity and all researches are

focusing on enhancing this parameter. The microcantilever operating in fluidic (gas or liquid) environments interacts with the surrounding fluid which causes a distributed mass depending on the fluid properties, frequency and cantilever width [22]. Thus, although the resonant frequency is an important parameter to mass density sensing, the structure's geometry and dimensions play an important role in the mass density sensitivity of microstructures. In the present work we study the effect of microcantilever shape (rectangular, U- and T-shaped microstructures) and geometrical dimensions on the gas mass density sensitivity (i.e., the ratio of resonant frequency variation to the density variation). To perform this study several uncoated silicon microcantilever shapes with different dimensions have been designed and fabricated. The structures have been tested at room conditions using different concentrations (0.2–2.0%) of hydrogen (H_2) in nitrogen (N_2). The density changes have been measured by monitoring the eigenfrequency (natural frequency) variation using the efficient phase linearization method [23].

2. Modeling

The Euler–Bernoulli equation taking into account the hydrodynamic force acting on the uncoated microcantilever is commonly used to model the behavior of resonating microcantilevers in fluid media when the influence of the beam's shearing deformation and rotational inertia can be neglected [8] and [12]. Fig. 1 displays the out-of-plane cantilever flexural mode (w is the free-end transverse deflection) and the geometric parameters: length (L), width (b) and thickness (h).

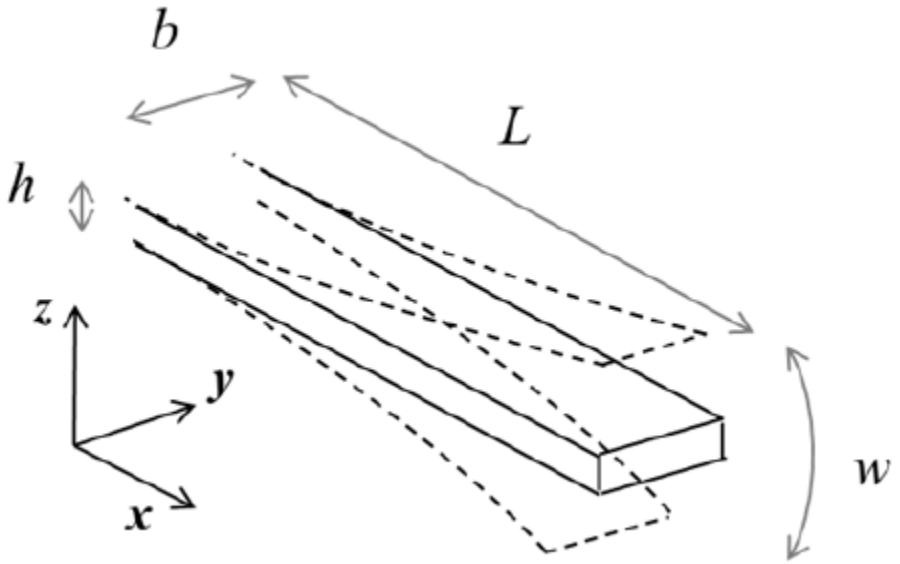

Fig.1 : Schematic representation of both the microcantilever geometry and the transverse bending deflection (*w*). The beam dimensions are width (*b*), length (*L*) and thickness (*h*).

In this work, the Euler–Bernoulli model in a fluid medium is used to characterize the changes in structural behavior due to the gas density variation. This model is valid only when [22]

- The beam has a uniform cross-section (geometry and materials) along the structure.
- The cross-sectional dimensions are negligible compared to the length of the structure: $h \ll b \ll L$.
- The deflection is negligible compared to the structural dimensions: $w \ll h$.

The solution of the differential equation governing the cantilever's motion in the presence of a surrounding fluid gives [22] and [24]:

$$\frac{df_0}{f_0} \simeq \frac{df_0}{f_{0,vac}} = -a_0 \frac{\pi}{8} \frac{b}{h} \frac{\rho_f}{\rho} \frac{d\rho_f}{\rho_f} \qquad (1)$$

with

$$f_{0,vac} = \frac{\lambda_n{}^2 h}{2\pi L^2}\sqrt{\frac{E}{12\rho}} \tag{2}$$

being the natural frequency in vacuum and f_0 the in-fluid natural frequency. Symbols E and ρ denote the Young's modulus and density of silicon, ρ_f is the fluid density, λ_n is a coefficient depending on the eigenfrequency mode [25] (λ_1 = 1.875, λ_2 = 4.695, λ_3 = 7.854, etc.), and a_0 = 1.0553. The latter parameter is associated with an approximation introduced by Maali et al. [24].

The absolute density sensitivity of resonating sensors is defined as the ratio between the resonant frequency variation and the density variation. Based on Eqs. (1) and (2), the absolute sensitivity can be written as

$$S_a = \left|\frac{\Delta f_0}{\Delta \rho_f}\right| = \frac{a_0}{\rho}\frac{b}{L^2}\frac{\lambda_n{}^2}{16}\sqrt{\frac{E}{12\rho}} \tag{3}$$

According to Eq. (3), it can be observed that the sensitivity of a rectangular beam, based on the Euler–Bernoulli assumption, depends only on two geometric parameters –- width (b) and length (L) –- and does not depend on the thickness (h). This result shows that changes in sensitivity need not be accompanied by changes in the resonant frequency. For example, increasing the width increases the sensitivity but does not affect the resonant frequency. It is expected from this equation that shorter and wider cantilevers will yield higher values of absolute sensitivity S_a. Of course, the range of applicability of Eq. (3) is limited to that of the Euler–Bernoulli theory on which it is based. Thus, an extreme reduction in length L would need to be accompanied by a corresponding reduction in thickness h in order to maintain the validity of Eq. (3); otherwise, the effects shear deformation and

Sensors and Actuators B: Chemical, Vol. 208 (March 2015): pg. 600-607. DOI.

rotational inertia, neglected in elementary beam theory, will become important. Such a reduction in *h* will also serve a more practical purpose: the use of shorter and wider cantilevers, which by Eq. (3) will improve the absolute sensitivity, will eventually become too stiff to render a measurable signal; reducing *h* will help to delay the onset of this practical limit to the applicability of Eq. (3).

3. Experiments

In order to experimentally study the optimization of the sensor sensitivity, several microcantilevers with different geometries (rectangular-, U- and T-shaped microstructures) and dimensions (*L*, *b* and *h*) have been fabricated (Fig. 2b; Table 1) with electromagnetic actuation and piezoresistive read-out (Fig. 2a).

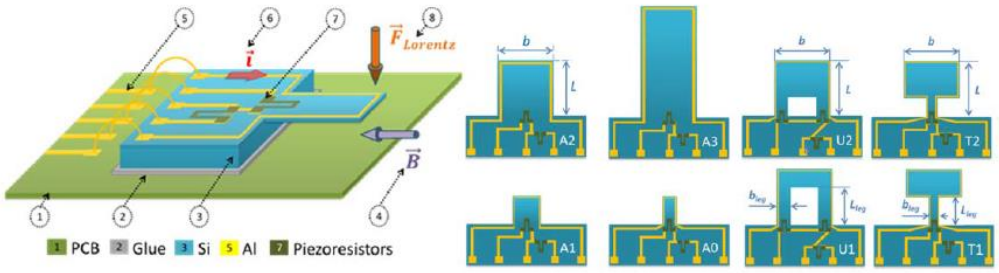

Fig.2 : (a) Uncoated silicon microcantilever design: (1) Printed Circuit Board, (2) adhesive, (3) silicon, (4) constant magnetic field, (5) metal, (6) AC current, (7) piezoresistor and (8) AC Lorentz force. **(b)** Different microcantilever geometries (rectangular-, U- and T-shaped) and geometric parameters: total length '*L*', total width '*b*', thickness '*h*', leg length '*Lleg*' and leg width '*bleg*'.

	[mm]		[µm]			[mm²]
Specimen	*L*	*b*	*h*	L_{Leg}	b_{Leg}	Surface
U1_5µ	1	1	5	666	250	0.670
U2_5µ	1	1	5	333	250	0.830
T1_5µ	1	1	5	500	200	0.600
T2_5µ	1	1	5	250	200	0.800
A0_5µ	0.5	0.25	5	-	-	0.125
A1_5µ	0.5	0.5	5	-	-	0.250
A2_5µ	1	1	5	-	-	1.000
A2_10µ	1	1	10	-	-	1.000
A3_5µ	2	1	5	-	-	2.000

Table 1: Microcantilever dimensions and surface areas. Extensions "_5μ" and "_10μ" indicate the specimen thickness in μm.

A gas line [23] has been used to generate different concentrations of H_2 in N_2 and to control the gas mixture flow. The different gas densities (ρ_{H2-N2}), gas density variations ($\Delta\ \rho_{H2-N2}$) and relative gas density variations ($\Delta\rho_f/\rho_f$) of the gas fluid (H_2–N_2) corresponding to different concentrations of H_2 in N_2 are reported in Table 2.

Concentrations of H_2 in N_2 (%)	$\rho_{H2\text{-}N2}$ (kg.m^{-3})	$\Delta\rho_{H2\text{-}N2}$ (kg.m^{-3} or g/l)	$\Delta\rho_f/\rho_f = \Delta\rho_{H2\text{-}N2}/\rho_{N2}$ (%)
100	0.0830	-1.0703	-93
2	1.1314	-0.0214	-1.8
1	1.1421	-0.0107	-0.93
0.6	1.1464	-0.0064	-0.56
0.2	1.1506	-0.0021	-0.19
0	1.1533	0	0

Table 2: Densities (ρ_{H2-N2}), density variations ($\Delta\ \rho_{H2-N2}$**)** and relative density variations ($\Delta\rho_f/\rho_f$) corresponding to different concentrations of H2/N2 gas mixture. These values are calculated at room conditions (23°C and 1.01325 bar).

3.1. Actuation and read-out systems

To actuate the cantilevers (Fig. 2a), an AC current is passed through the conductive loop wire placed along the cantilever periphery. In the presence of a magnetic field collinear to the longitudinal axis of the beam, an AC Lorenz force is created at the microcantilever free-end and induces out-of-plane vibrations (Fig. 1). Semiconductor strain gauges which are boron-doped piezoresistors have been fabricated during the process in order to read-out the vibrations. They are arranged in a half Wheatstone bridge configuration: a first gauge is located at the clamped-end of the beam where the strain is maximum and the second one is on the rigid substrate.

3.2. Microcantilever fabrication

The main steps of the fabrication process are as follows. The starting substrate was a 100 mm-diameter, 〈1 0 0〉, N-type silicon-

on-insulator (SOI) wafer, with a 1 μm-thick buried oxide and a 5 μm-thick (or 10 μm-thick) top silicon layer (resistivity of 4–6 Ω cm). The use of the SOI wafer enabled the precise control of the cantilever thickness, ensuring the consistency of their mechanical properties. The first step consisted of creating the piezoresistor in the bulk silicon. In order to optimize the piezoresistor sensitivity, the cantilevers were patterned along crystal axes for which the longitudinal piezoresistive coefficient is maximum, i.e., along the 〈1 1 0〉 direction in the case of a *p*-silicon piezoresistor. The fabrication method relied on the implantation of germanium (Ge) and boron fluorine (BF_3) in order to obtain an ultrathin piezoresistor [26]. The localization of the piezoresistive layer at the anchored edge of the cantilevers was achieved by using silicon dioxide as a masking layer. For that purpose, 300 nm of silicon dioxide was thermally grown and patterned with a photolithographic step. Germanium was implanted with an energy of 60 keV and a dose of 5×10^{14} ions/cm^2 through a 6-nm silicon dioxide layer to create a preamorphized layer. This layer avoided channeling effects during the boron implantation and led to a very thin doped region. Boron fluorine was then implanted with an energy of 15 keV and a dose of 1×10^{16} ions/cm^2. Owing to the heavier mass of the BF_3 molecules relative to boron, the use of BF_3 resulted in a thickness reduction of the p^+-doped region. The implantation process was followed by rapid thermal annealing at 1000 °C for 15 s to minimize boron diffusion during the recrystallization of the amorphized layer and the electrical activation. This was followed by conventional annealing at 850 °C during 20 min. The next step consisted of the deposition of 200 nm of plasma enhanced chemical vapor deposition (PECVD) silicon dioxide on the entire SOI wafer before the sputtering of aluminum (Al) (500 nm) for the electrode used for electromagnetic actuation. The oxide prevented shortcircuiting between the piezoresistors and the actuation electrodes. Lift-off of the Al film was achieved by using an AZ nLOF negative photoresist to define the electrodes. A passivation silicon oxide film (200 nm thick) was then deposited by PECVD. Contact pads were opened by dry etching of PECVD-deposited oxide. To finish, the microcantilever shapes were defined by a front reactive ion etching of silicon, followed by vertical sidewalls etching on the backside of the SOI wafer using the deep reactive ion etching technique to release the structures. The 1 μm-thick SiO_2 acted as an etch stop layer for the dry silicon etching. This layer was then removed

by Reactive ion etching. The resulting microstructural shapes, dimensions and surface areas are reported in Table 1.

3.3. Experimental setup

With the aim of comparing the different microcantilever geometries and dimensions in terms of sensitivity to density variation, measurements of various H_2 in N_2 concentrations (0.2, 0.6, 1 and 2%) have been performed using a gas line with a flow of 100 ml/min. The hermetic cell containing the tested microcantilever had a volume of 500 µl. A gain/phase analyzer (HP4194A) controlled with a *LabVIEW* program was used to acquire the phase spectrum every nine seconds (1 acquisition/9 s). In order to measure the natural frequency variation (Δf_0), a linearization of the phase spectrum around the resonance was used to extract the natural frequency (f_0) as detailed in [23].

The study of both the geometry and the size influence on the sensor sensitivity was performed with tests using the first resonant mode of each structure. The first step of the study consisted of determining the structural shape influence (rectangular-, U- or T-shaped) by comparing the sensitivities of the structures A2_5µ, T1_5µ, T2_5µ, U1_5µ and U2_5µ, all having the same total length (L), total width (b) and thickness (5 µm). The second step involved an investigation of the influence of the dimensions (L, b and h) on the sensitivity for the best sensitive shape (geometry) revealed by the results of the first step. An example of the measurement performed for each microstructure of Table 1 is presented in Fig. 3.

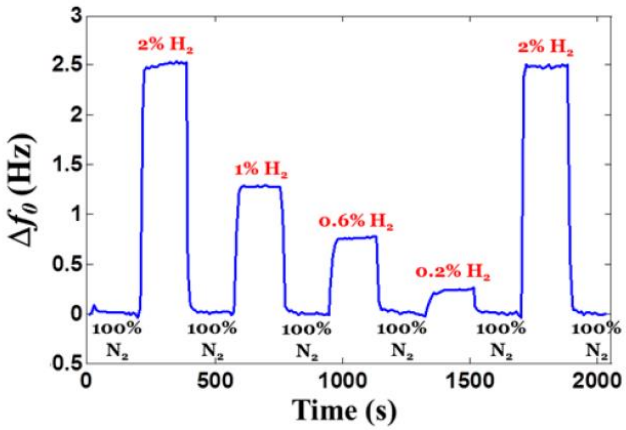

Fig. 3: Example of detection curve obtained using A2_5µ structure with different concentrations of H_2 in N_2 with a gas flow of 100 ml/min at room conditions (Temperature≈23°C, pressure≈1 atm).

The optimization was performed by consideration of the absolute sensitivity defined in Eq. (3). Other sensor characteristics and performance metrics were also determined using the hydrogen detection measurements:

- The sensor noise (*Noise*) has been estimated by the standard deviation on the stabilized natural frequency ($\Delta f_0 \approx 0$)
- The signal-to-noise ratio (*SNR*) and the eigenfrequency variation (Δf_0) have been calculated at 1% of H_2 in N_2.
- The limit of detection (*LOD*) has been estimated: it corresponds to a signal-to-noise ratio equal to 3.
- The absolute sensitivity is the slope of the fitted line of the experimental measurements.

4. Results and discussion

4.1. Experiment set #1: influence of the shape

This first experiment set was used for the first step of the sensitivity study consisting of the examination of the shape influence (rectangular-, T- or U-shaped structure) on the sensitivity. Fig. 4a and b shows the experimental measurements (markers) and the fitting lines of the first-mode natural frequency variation as a function of H_2 in N_2 concentration and density variation, respectively. The A2_5µ structure has the highest sensitivity (slope) among all of the other structures considered, namely U1_5µ, U2_5µ, T1_5µ and T2_5µ. The performance metrics are presented in Fig. 4c and the numerical results are reported in Table 3.

This preliminary result allows us to conclude that for structures having the same total length (*L*), the same total width (*b*) and the same thickness (*h*), structures having more contact area (Table 1) with the surrounding fluid have the best absolute sensitivity (S_a) to the density variations of the surrounding gas (Fig. 4b; Table 3). This is a simplistic conclusion because structures having more contact area and keeping the same total length (*L*), total width (*b*) and total thickness

(*h*), also have higher resonant frequency. According to these first experiments, we can conclude that the rectangular shape (A2_5µ in these experiments) is the best geometry in terms of sensitivity for gas density sensing applications. It can be seen in Fig. 4c that the A2_5µ structure also has the best quality factor (*Q*) and the best signal-to-noise ratio (*SNR*) and, thus, the best limit of detection (*LOD* = 100 ppm or 0.11 mg/l).

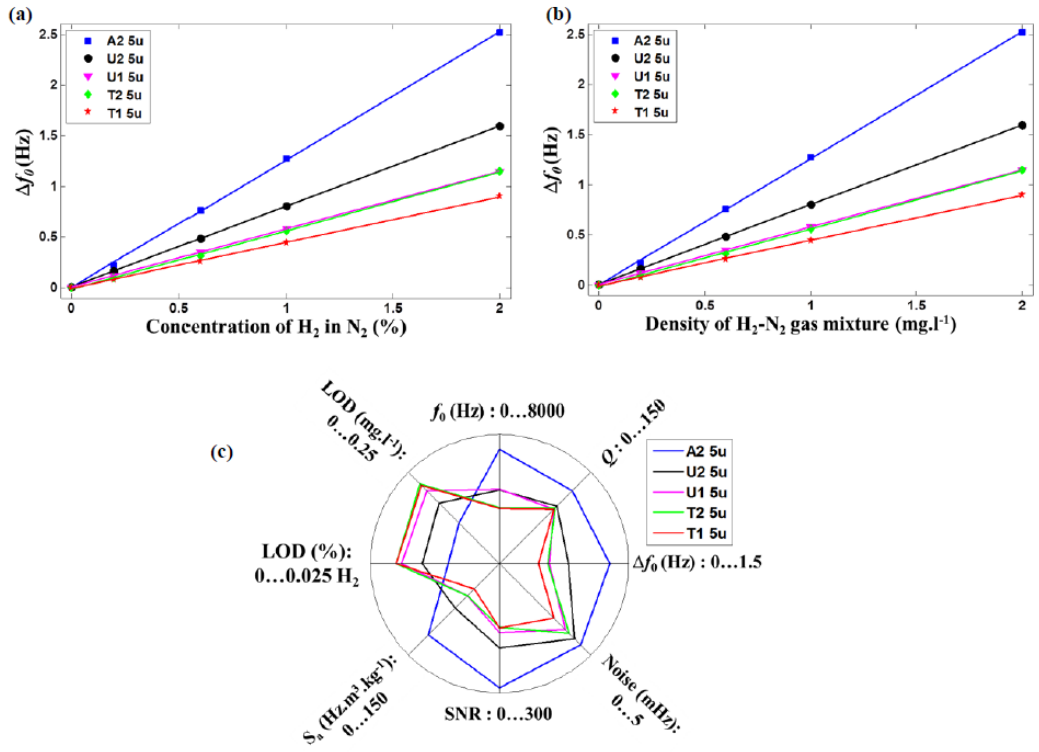

Fig. 4: Results of the first experiments. (a) Natural frequency variation as function of H_2 in N_2 concentration (0, 0.2, 0.6, 1 and 2%). (b) Natural frequency variation as function of the density variation of the H2-N2 gas mixture. (c) Performance of structures A2_5µ, U1_5µ, U2_5µ, T1_5µ and T2_5µ in terms of natural frequency (f_0), quality factor (Q), natural frequency variation (Δf_0) at 1% of H_2 in N_2, noise (*Noise*) estimated by the calculation of the standard deviation, signal-to-noise ratio (*SNR*) calculated at 1% of H_2 in N_2, absolute sensitivity (S_a) which is the slope of the linear characteristics and limit of detection (*LOD*) in terms of H_2 in N_2 concentration (%) and density variation ($mg.l^{-1}$).

Sensors and Actuators B: Chemical, Vol. 208 (March 2015): pg. 600-607. DOI.

Specimen	f_0 (Hz)	Q	Δf_0 (Hz)	*Noise* (mHz)	*SNR*	S_a (Hz.kg^{-1}.m^3)	*LOD* (%)	*LOD* (mg.l^{-1})
A2_5µ	7082	120	1.28	4.43	289	117	0.01	0.11
U2_5µ	4580	94	0.80	4.1	195	73	0.015	0.16
U1_5µ	4624	90	0.58	3.6	161	53	0.019	0.20
T2_5µ	3480	92	0.56	3.80	147	53	0.02	0.22
T1_5µ	3431	90	0.45	3	150	42	0.02	0.21

Table. 3 : Numerical values of performance metrics extracted from the experiments made with A2_5µ, U2_5µ, U1_5µ, T2_5µ and T1_5µ structures.

4.2. Experiment set #2: influence of the dimensions

The previous experiments have shown that, for the same overall dimensions, the rectangular structures are the best geometries in terms of sensitivity to the gas density changes. In this section we therefore study the effect of the geometric parameters (*L*, *b* and *h*) on the sensitivity of rectangular structures by analyzing the structural responses to the different concentrations of H_2 in N_2.

4.2.1. Thickness influence

The structures A2_5µ and A2_10µ have the same length and width (*L*, *b*) with thicknesses (*h*) of 5 µm and 10 µm, respectively. The detection curves of both structures are presented in Fig. 5a and b where it can be seen that thickness has no effect on the absolute sensitivity (S_a) (red triangle and green diamond markers). The fact that the absolute sensitivity is independent on the thickness is consistent with Eq. (3). Furthermore, doubling the thickness doubles the quality factor as can be seen in Table 4.

4.2.2. Length and width influence

Keeping in mind that the primary goal is to identify the best structure in terms of sensitivity to gas density, this part has three objectives:

- Objective 1 consists of comparing the geometries A2_5µ and A3_5µ in terms of their absolute sensitivity (S_a). These structures have been selected because they have the same

widths and thicknesses, but A3_5μ is two times longer than A2_5μ.

- Objective 2 involves the sensitivity comparison between the geometries A1_5μ and A0_5μ having the same lengths and thicknesses, but A1_5μ is two times wider than A0_5μ.
- Objective 3 is to compare sensitivities of the two square geometries A1_5μ and A2_5μ having the same thickness, but the second structure has length and width two times larger than the first one.

The structural dimensions are reported in Table 1. Fig. 5 summarizes the detection results obtained with the different geometries and Table 4 reports the numerical characteristics and performance metrics of the different sensors. Performing in order the three comparisons mentioned above, the experimental results demonstrate the following:

- For a fixed width, the shorter beams have higher absolute sensitivities.
- For a fixed length, the wider beams have higher absolute sensitivities.
- When the width and length are both halved, the structure's sensitivity is increased by a factor of approximately two.

These points confirm the scale effects indicated by Eq. (3), which shows that the absolute sensitivity is proportional to the ratio of width to the square of the length (b/L^2).

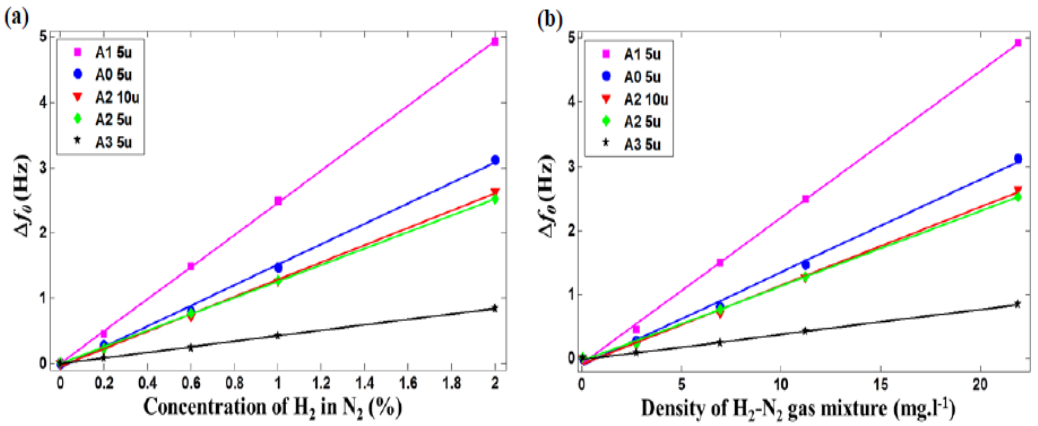

Sensors and Actuators B: Chemical, Vol. 208 (March 2015): pg. 600-607. DOI.

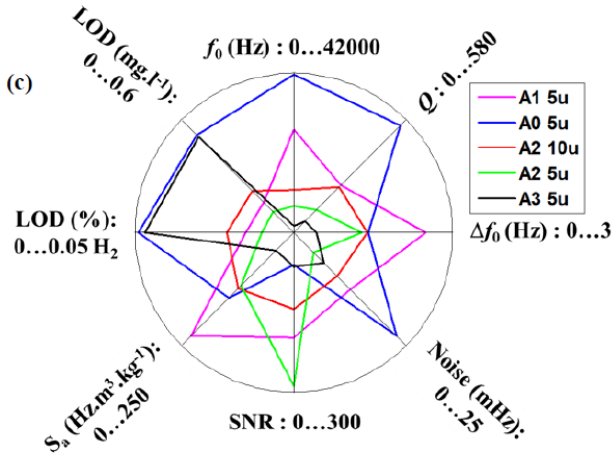

Fig. 5: Results of the second set of experiments. (a) Natural frequency variation as function of H_2 in N_2 concentration (0, 0.2, 0.6, 1 and 2%). (b) Natural frequency variation as function of the density variation of the H_2-N_2 gas mixture. (c) Performance of structures A1_5µ, A0_5µ, A2_10µ, A2_5µ and A3_5µ in terms of: natural frequency (f_0), quality factor (Q), natural frequency variation (Δf_0) at 1% of H_2 in N_2, noise (*Noise*) estimated by the calculation of the standard deviation, signal-to-noise ratio (*SNR*) calculated at 1% of H_2 in N_2, absolute sensitivity (S_a) which is the slope of the fitted straight lines and limits of detection (*LOD*) in terms of H_2 in N_2 concentration (%) and density variation ($mg.l^{-1}$).

Specimens	f_0 (Hz)	Q	Δf_0 (Hz)	*Noise* (mHz)	*SNR*	S_a ($Hz.kg^{-1}.m^3$)	*LOD* (%)	*LOD* ($mg.l^{-1}$)
A0_5µ	41700	570	1.40	22.83	61	145	0.049	0.52
A1_5µ	27099	250	2.50	12.60	198	228	0.015	0.16
A2_5µ	7082	120	1.28	4.43	289	117	0.010	0.11
A2_10µ	11260	240	1.38	9.55	145	123	0.021	0.22
A3_5µ	1760	60	0.43	6.77	64	39	0.047	0.51

Table. 4: Numerical performance values extracted from the experiments made with A0_5µ, A1_5µ, A2_5µ, A0_10µ and A3_5µ structures.

We note that all structures (experiment sets #1 and #2) detect 0.2% of H_2 in N_2, corresponding to 2 mg/l as density variation. Furthermore, we announce a theoretical detection limit (*LOD*) of 0.01% (100 ppm) of H_2 in N_2 corresponding to 0.11 mg/l as density variation for the A2_5µ structure, which is 800 times smaller than the published value of Rosario et al. [7]. We also note that this limit of detection can be improved considerably by increasing the actuation force.

Sensors and Actuators B: Chemical, Vol. 208 (March 2015): pg. 600-607. DOI.

4.3. Theory vs. experiment

In the literature there are no theoretical models that permit one to accurately predict the resonant frequency variation due to fluid density change for the case of complex geometries such as T-shaped, U-shaped and V-shaped cantilevers. The only existing model concerns parallelepiped-cantilever (rectangular) geometries that respect the Euler–Bernoulli conditions listed in Section 2. Therefore, only rectangular-shaped microcantilevers are considered for this comparison although their dimensions do not always respect the Euler–Bernoulli conditions.

In Fig. 6 comparisons are made between the model [Eqs. (1) and (2)] and measurements of natural frequency (f_0) and natural frequency variation (Δf_0) at 1% of H_2 in N_2.

We observe in Fig. 6a that the accuracy of the theoretical model in terms of f_0 estimation is satisfactory with the exception of the A0_5μ structure having a relative error of 25%. This error is most likely due to the structure etching defects [27] which have substantially modified the length of the cantilever (reduction). The evidence is provided by the fact that the structure A3_5μ, having exactly the same shape ($L = 2b$) as the A0_5μ structure but with a size four times larger (Table 1), shows good agreement between measurement and theory.

It can be observed in Fig. 6b that the relative deviation between model and measurement for the frequency shift estimation is about 50% for all structures except A3_5μ. These relatively high deviations are due to the fact that the microcantilevers do not respect the Euler–Bernoulli conditions; thus, the fluid-structure interaction model proposed by Sader et al. [22] is not expected to give a good approximation. The A3_5μ structure is two times longer than its width ($L = 2b$) and therefore has a smaller relative deviation (31%) than the other cases since the model is expected to be more applicable for longer geometries. The A0_5μ structure has a larger error (46%) than A3_5μ (31%) for the same reason mentioned in the previous paragraph.

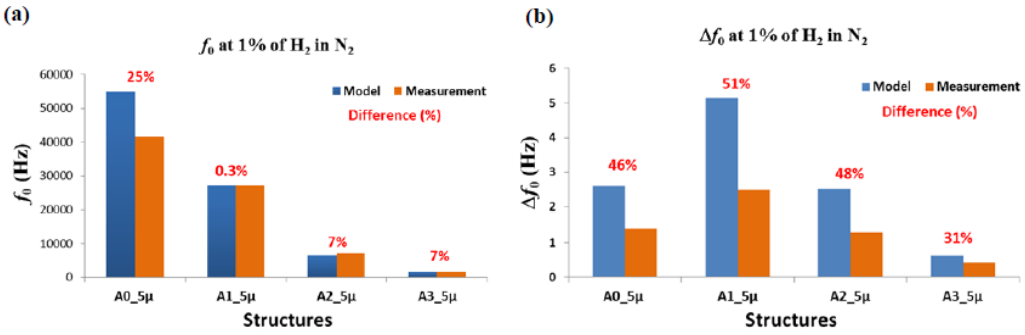

Fig. 6: Comparison between model and measurements at 1% of H_2 in N_2. (a) Natural frequency (f_0). (b) Natural frequency variation (Δf_0).

In order to verify the effect of geometry in modeling accuracy, another measurement has been realized at the same room conditions (temperature = 23 °C, pressure = 1 atm) and gas conditions (H_2–N_2: 0.2–2%, gas flow = 100 ml/min) using another microcantilever ($L \times b \times h$ = 2000 µm × 400 µm × 5 µm) having a length five times greater than its width ($L = 5 \times b$).

The frequency-shift results of this experiment are reported in Fig. 7 from which we see that the relative deviation between the model and the measurement for 1% of H_2 in N_2 is 3.12%. This result confirms that the Euler–Bernoulli conditions must be respected in order to achieve a good estimate using Sader's model [22] (or any model based on elementary beam theory). We also remark that the error increases for lower concentrations (0.6% and 0.2% in Fig. 7). The reason is the relatively large frequency step between each measurement caused by the relatively large span measurement in this case (20 Hz). In fact, the gain-phase analyzer (HP4194A) has a maximum of 400 measurement points; thus, configuring a span measurement of 20 Hz for the acquisition of the gain and phase spectra, a 50-mHz frequency step is achieved. However, using the phase linearization method [23], the resonant frequency can be estimated with a better accuracy than the frequency step.

Sensors and Actuators B: Chemical, Vol. 208 (March 2015): pg. 600-607. DOI.

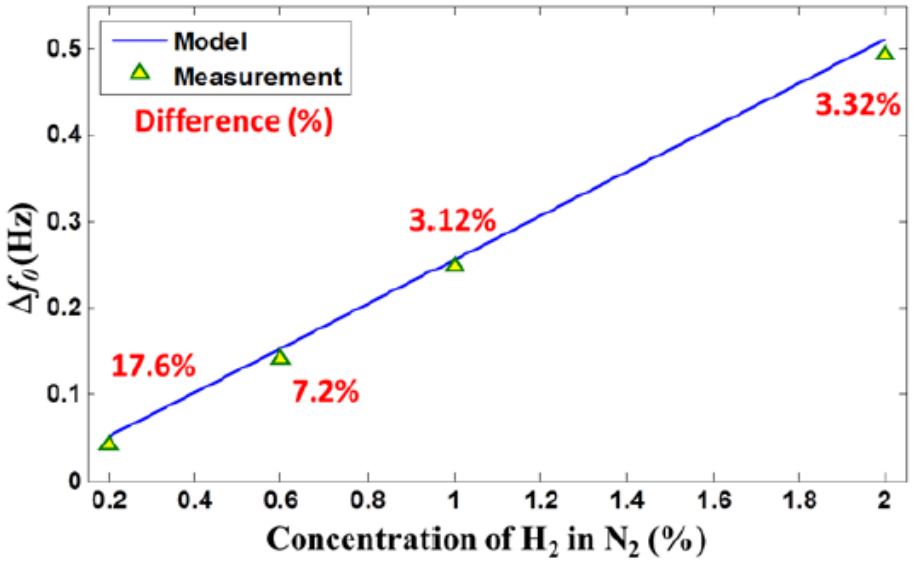

Fig. 7: Measurement of concentration of H_2 in N_2 (0.2-2%) with gas flow of 100 ml/min using rectangular-shaped microcantilever (L x b x h= 2000 x 400 x 5μm^3). The triangle markers present experimental measurements, the blue line presents the theoretical modeling [Eq. (3)] and the red numerical values present the relative deviation between model and measurements.

5. Conclusions

We have demonstrated that uniform rectangular cantilevers are more suitable for density measurement than the other tested T- and U-shapes. Moreover, wide and short beams are more sensitive to the density variation, with the sensitivity of the rectangular beams being proportional to b/L^2. Furthermore, the thickness does not affect the sensitivity of rectangular cantilevers to the mass density changes despite the fact that it affects the resonant frequency. However, the noise on the resonant frequency estimation depends on the thickness of the microcantilever. Thus, in order to select the most appropriate thickness for a given structure size (length and width) in view of limit-of-detection optimization, noise consideration has to be studied.

We have also modeled the fluid-structure interaction using the Euler–Bernoulli beam model combined with the hydrodynamic force. This modeling shows good agreement with measurements when the rectangular structures are narrow and sufficiently long (length ≥ 5 × width in our case). These results may help designers to

Sensors and Actuators B: Chemical, Vol. 208 (March 2015): pg. 600-607. DOI.

optimize the cantilever geometry and dimensions in order to be more or less sensitive to the gas density variation depending on the application.

Moreover, due to the implementation of the phase linearization method [23] used to estimate the small natural frequency variation, detection of 2 mg/l of the gas mass density change has been achieved with all the microstructures and a limit of detection of 0.11 mg/l of the gas mass density variation (corresponding to a concentration of 100 ppm of H_2 in N_2) has been estimated, which is much smaller than the previous state-of-the-art value of 88 mg/l [7].

6. Acknowledgment

The authors gratefully acknowledge the French National Radioactive Waste Management Agency (Andra, F-92298 Châtenay-Malabry, France. http://www.andra.fr/) for their support of this research. Grant number: UBX-Andra 055221 collaboration agreement.

7. References

1. C. Vančura, Y. Li, J. Lichtenberg, K.U. Kirstein, A. Hierlemann, F. Josse, Liquid-phase chemical and biochemical detection using fully integrated magnetically actuated complementary metal oxide semiconductor resonant cantilever sensor systems, Analytical Chemistry, 79 (2007), pp 1646-1654.

2. K. M. Goeders, J. S. Colton, L. A. Bottomley, Microcantilevers: Sensing chemical interaction via mechanical motion, Chemical review, 108 (2008), pp 522-542.

3. A. Boisen, S. Dohn, S.S. Keller, S. Schmid, M. Tenje, Cantilever-like micromechanical sensors, Reports on Progress in Physics, 74 (2011) 036101.

4. Johnson, R. Mutharasan, Biosensing using dynamic-mode cantilever sensors: a review, Biosensors and bioelectronics, 32 (2012), pp 1-18.

5. X. Li, D.W. Lee, Integrated microcantilevers for high-resolution sensing and probing, Measurement,Science and Technology., 23 (2012), 022001 (40 pages).

6. Q. Zhu, Microcantilever sensors in biological and chemical detections, Sensors & transducers,125 (2011), pp 1-21.

7. R. Rosario, R. Mutharasan, Piezoelectric excited millimeter sized cantilever sensors for measuring gas density changes, Sensors and Actuators B, 192 (2014), pp 99–104.

8. S. Tétin, B. Caillard, F. Ménil, H. Debéda, C. Lucat, C. Pellet, I. Dufour, Modeling and performance of uncoated microcantilever-based chemical sensors, Sensors and Actuators B 143 (2010) 555–560.

9. L. Zhao, L. Xu, G. Zhang, Z. Jiang, Y. Zhao, J. Wang, X. Wang, Z. Liu, In-situ measurement of fluid density rapidly using a vibrating piezoresistive microcantilever sensor without resonance occurring, IEEE sensors Journal, 14 (2014), pp 645-650.

10. E. Lemaire, B. Caillard, M. Youssry, I. Dufour, High-frequency viscoelastic measurements of fluids based on microcantilever sensing: New modeling and experimental issues, Sensors and Actuators A, 201 (2013), pp 230– 240.

11. B. A. Bircher, L. Duempelmann, K. Renggli, H. P. Lang, C. Gerber, N. Bruns, T. Braun, Real-time viscosity and mass density sensors requiring microliter sample volume based on nanomechanical resonators, Analytical Chemistry, 85 (2013), pp 8676−8683.

12. M.T. Boudjiet, V. Cuisset,, C. Pellet, J. Bertrand,, I. Dufour, Preliminary results of the feasibility of hydrogen detection by the use of uncoated silicon microcantilever-based sensors, International Journal of Hydrogen Energy (2014), http://dx.doi.org/10.1016/j.ijhydene.2014.03.228

13. A. Kramer, Th. A. Paul, High-precision density sensor for concentration monitoring of binary gas mixtures, Sensors and Actuators A, 202 (2013), pp 52-56.

14. D. Sparks, R. Smith, J. Patel, N. Najafi, A MEMS-based low pressure, light gas density and binary concentration sensor, Sensors and Actuators A, 171 (2011), pp 159– 162.

15. A. Loui, F.T. Goericke, T.V. Ratto, J. Lee, B.R. Hart, W.P. King, The effect of piezoresistive microcantilever geometry on cantilever sensitivity during surface stress chemical sensing, Sensors and Actuators A, 147 (2008), pp 516–521.

16. H. Hocheng, W.H. Weng, J.H. Chang, Shape effects of micromechanical cantilever sensor, Measurement, 45 (2012), pp 2081–2088.

17. S. Subramanian, N. Gupta, Improved V-shaped microcantilever width profile for sensing applications, Appl. Phys. 42 (2009), 185501.

18. M. Z. Ansari, C. Cho, Deflection, frequency, and stress characteristics of rectangular, triangular, and step profile microcantilevers for biosensors, Sensors, 9 (2009), pp 6046-6057.

19. M. Narducci, E. Figueras, M. J. Lopez, I. Gràcia, J. Santander, P. Ivanov, L. Fonseca, C. Cané, Sensitivity improvement of a microcantilever based mass sensor, Microelectronic Engineering, 86 (2009), pp 1187–1189.

20. S. Morshed, B. C. Prorok, Enhancing the sensitivity of microcantilever-based sensors via geometry modification, Proc. SPIE 6223, Micro (MEMS) and Nanotechnologies for Space Applications, 62230S (2006), pp1-9.

21. L.A. Beardslee, F. Josse, S.M. Heinrich, I. Dufour, O. Brand, Geometrical considerations for the design of liquid-phase biochemical sensors using a cantilever's fundamental in-plane mode, Sensors and Actuators B, 164 (2012), pp 7– 14.

22. J.E. Sader, Frequency response of cantilever beams immersed in viscous fluids with applications to the atomic force microscope, Journal of applied physics, 84 (1998), pp 64-76.

23. M.T. Boudjiet, J. Bertrand, C. Pellet, I. Dufour, New characterization methods for monitoring small resonant frequency variation: Experimental tests in the case of hydrogen detection with uncoated silicon microcantilever-based sensors, Sensors and Actuators B 199 (2014) 269–276.

24. A. Maali, C. Hurth, R. Boisgard, C. Jai, T. C. Bouhacina, J.-P. Aimé, Hydrodynamics of oscillating atomic force microscopy cantilevers in viscous fluids, Journal of Applied Physics, 97 (2005), pp 074907-1-6.

25. R. D. Blevins, Formulas for natural frequency and mode shape, Van Nostrand Reinhold, 1979.

26. C. Bergaud, E. Cocheteau, L. Bary, R. Plana, and B. Belier, Formation of implanted piezoresistors under 100-nm thick for

nanoelectromechanical systems, Proc. 15th IEEE Int. Conf. Micro Electro Mech. Syst., (2002), pp 360–363.

27. L. Fadel-Taris, C. Ayela, F. Josse, S.M. Heinrich, D. Saya, O. Brand, I. Dufour , Influence of non-ideal clamping in microcantilever resonant frequency estimation, FCS, Joint Conference of the IEEE International (2011), pp 1-5.

About the Authors

M.T. Boudjiet : Univ. Bordeaux, IMS, UMR 5218, F-33400 Talence, France

Tel.: +33 (0) 5 40 00 27 09.

Email:

mohand-tayeb.boudjiet@ims-bordeaux.fr

Vitae: Mohand-Tayeb Boudjiet received in 2012 the Master's degree in embedded electronics systems from University of Bordeaux in France. He is currently a Ph.D. student at IMS Laboratory working on microcantilevers for density measurement and chemical detection.

J. Bertrand : Andra, F-92298 Châtenay-Malabry, France

Vitae: Johan Bertrand received in 2005 the M.S. degree in solid and inorganic chemistry from Rennes 1 University, France. In 2009, he earned his Ph.D. degree in physics and chemistry from the University of Tubingen and École des Mines de Saint-Étienne. Since 2009, he works for the National Radioactive Waste Management Agency as a Research Engineer on the development of an overall monitoring strategy and sensors development for the deep geological disposal of high-level and long-lived radioactive waste.

F. Mathieu : CNRS, LAAS, F-31077 Toulouse, France

Vitae: Fabrice Mathieu was born in Orléans, France, in 1972. He received the Engineer degree in communication systems and electronics from the CNAM (Conservatoire National des Arts et Métiers), Toulouse, France, in 2003. He joined the Laboratoire d'Analyse et d'Architecture des Systèmes (LAAS), Center National de la Recherche Scientifique (CNRS), Toulouse, in 2001, where he is currently in charge of the development and the design of very low signal detection systems applied to the micro(nano)electromechanical systems area and its complete electronic treatment and control for automation.

L. Nicu : Andra, F-92298 Châtenay-Malabry, France

Vitae: Liviu Nicu was born in 1973 in Bucharest (Romania). After completing his Master of Electrical Engineering at the Paul Sabatier University of Toulouse (France) in 1997, he joined the Integrated Microsystems Group at the LAAS (Laboratory for Analysis and Architecture of Systems) of Toulouse where he obtained his Ph.D. in 2000 into the Micromechanical Structures field. From 2000 to 2003, he was R&D Engineer at Thales Avionics, Valence (France). His activities focused onto the development of micromechanical sensors for the civil and military navigation applications. Since 2003 he joined the NanoBioSytems Group at LAAS as a full time CNRS (National Center of Scientific Research) researcher where he currently works in two main research fields: the development of (1) new resonant bio(chemical)sensors using M(N)EMS technologies and of (2) cantilever-

based microsystems for contact deposition of small amounts of biological samples for biochip applications.

L. Mazenq : Andra, F-92298 Châtenay-Malabry, France

Vitae: Laurent Mazenq was born on May 30, 1982. He received his University Institute of Technology's Degree from the University Paul Sabatier de Toulouse (France) in 2002. Then, he joined the Laboratoire d'Analyse et d'Architecture des Systèmes of the French Center National de la Recherche Scientifique (LAAS-CNRS) as an Engineer Assistant. In 2011, he joined Freescale Semiconductor (France) in production process Engineering. He is working on UV projection lithography.

T. Leïchlé : Andra, F-92298 Châtenay-Malabry, France

Vitae: Thierry Leïchlé is a CNRS researcher at the Laboratory for Analysis and Architecture of Systems in Toulouse (France). He obtained his M.S. from the Georgia Institute of Technology, Atlanta (USA), in 2002 and his Ph.D. from the University of Toulouse III in 2006. From 2007 to 2009 he was a postdoctoral fellow at the Institute of Physics, Academia Sinica, Taipei (Taiwan).

S.M. Heinrich : Department of Civil, Construction and Environmental Engineering, Marquette University, Milwaukee, WI, USA

Vitae: Stephen M. Heinrich earned his B.S. from Penn State in 1980 and his M.S. and Ph.D. degrees from the University of Illinois in 1982 and 1985, all in civil engineering. He then joined the faculty at Marquette University where he is currently Professor of Civil Engineering. Dr. Heinrich's research has focused on

structural mechanics applications in microelectronics packaging and the development of new analytical models for predicting/enhancing the performance of cantilever-based chemical sensors. The work performed by Dr. Heinrich and his colleagues has resulted in over 100 publications/presentations and three best-paper awards from IEEE and ASME.

C. Pellet : Univ. Bordeaux, IMS, UMR 5218, F-33400 Talence, France

Vitae: Claude Pellet was a researcher at the "Institut d'Electronique Fondamentale" from the University of Paris XI-Orsay, where he studied the deposition of thin films by ion beam sputtering from 1982 to 1993. He joined University of Bordeaux as a full professor in 1993. His work focuses on micro-technology, micro-system development (humidity sensors), assembly technology and micro-systems reliability. He is currently the director of the IMS Laboratory, overseeing a staff of 400 people.

I. Dufour : Univ. Bordeaux, IMS, UMR 5218, F-33400 Talence, France

Vitae: Isabelle Dufour graduated from Ecole Normale Supérieure de Cachan in 1990 and received the Ph.D. and H.D.R. degrees in engineering science from the University of Paris-Sud, Orsay, France, in 1993 and 2000, respectively. She was a CNRS research fellow from 1994 to 2007, first in Cachan working on the modeling of electrostatic actuators (micromotors, micropumps) and then after 2000 in Bordeaux working on microcantilever-based chemical

Sensors and Actuators B: Chemical, Vol. 208 (March 2015): pg. 600-607. DOI.

sensors. She is currently Professor of electrical engineering at the University of Bordeaux and her research interests are in the areas of microcantilever-based sensors for chemical detection, rheological measurements, materials characterization and energy harvesting.